e-ISSN: 3023-7343

TETHYS ENVIRONMENTAL SCIENCE
an International Journal

CMIP6-Constrained Machine Learning Assessment of Pre-Monsoon Rainfall Variability and Near-Term Projection in Selected Districts of Telangana, India

Gollamandala Jeevana Mounika[1,4], Gubbala China Satyanarayana[2], Sambasivarao Velivelli[3], Chennu Venkata Naidu[1], Anil Kumar Medikonda[1,*], Mallela Pruthvi Raju[1]

[1]Department of Meteorology and Oceanography, Andhra University, 530003 Andhra Pradesh, India. [2]National Institute of Disaster Management (NIDM), South Campus, 521212 Andhra Pradesh, India. [3]Center for Atmospheric Science, Department of Electronics and Communication Engineering, Koneru Lakshmaiah Education Foundation, 522302 Guntur, India. [4]Government Degree College, Chintalapudi, Eluru District, 534460 Andhra Pradesh, India.

Research Article

Citation: Mounika, G. J., Satyanarayana, G. C., Velivelli, S., Naidu, C. V., Medikonda, A. K., Raju, M. P. (2026). CMIP6-Constrained Machine Learning Assessment of Pre-Monsoon Rainfall Variability and Near-Term Projection in Selected Districts of Telangana, India. *Tethys Env. Sci.* 3(1): 54-69.

DOI: 10.71350/tethysjournal.6

Received: 10 May 2026

Accepted: 23 June 2026

Available Online: 28 June 2026

Publication Date: 29 June 2026

Abstract

Pre-monsoon (March-May; MAM) rainfall over Telangana is highly variable, yet district-scale evidence on its variability, extremes, and near-term change remains limited. This study combines India Meteorological Department gridded rainfall observations (1951-2024), bias-corrected NEX-GDDP-CMIP6 simulations, and machine-learning (ML) post-processing to examine MAM rainfall in six contrasting districts: Adilabad, Nizamabad, Karimnagar, Hyderabad, Mahabubnagar, and Khammam. Observations show strong spatial heterogeneity, with coefficients of variation from 60.2% in Hyderabad to 83.0% in Khammam. Trend decomposition indicates that recent changes are more closely linked to increasing rainfall intensity than wet-day frequency; the strongest seasonal trends occur in Nizamabad and Khammam (about 0.32 mm yr^{-1}), although statistical significance is spatially limited. Twenty CMIP6 models were evaluated using a composite performance index based on correlation, normalized error, variability ratio, and bias. The five best-performing models, CMCC-ESM2, ACCESS-ESM1-5, TaiESM1, MRI-ESM2-0, and INM-CM5-0, were retained for ML post-processing. Random Forest, XGBoost, and LSTM showed comparable skill during independent testing, but LSTM produced more stable district-wise correlations while still underestimating peak rainfall years. Under SSP5-8.5, LSTM-based projections for 2031-2050 indicate changes from -5.2% in Nizamabad to +36.4% in Adilabad relative to 1981-2010, supporting localized interpretation rather than broad generalization for regional climate-risk assessment and adaptation planning practice.

Keywords: *Pre-monsoon rainfall, Telangana, CMIP6, machine learning, LSTM, SSP5-8.5.*

Correspondence: Anil Kumar Medikonda
dranilmedi@gmail.com

Introduction

Pre-monsoon rainfall during March-May (MAM) is a small but important component of the hydroclimatic cycle over peninsular India. It supplies early-season moisture after the dry winter period, affects sowing decisions and groundwater recharge, and can temporarily moderate late-spring heat stress in semi-arid regions (Kumar et al., 2004; Gadgil and Gadgil, 2006). Because this rainfall is often produced by localized convective storms and mesoscale disturbances, its spatial variability is high, and regional averages may obscure local risk.

Telangana, located on the Deccan Plateau, contains strong contrasts between relatively wetter northern and eastern districts, urban-influenced central areas, and drought-prone southern districts. These contrasts are relevant to agriculture, water-resource planning, and flash-flood risk, especially in rapidly urbanizing areas such as Hyderabad. Although Indian monsoon variability and extreme rainfall have been widely studied at national and regional scales, including assessments of regional climatic controls (Krishnan et al., 2020), district-scale evidence for pre-monsoon rainfall variability, extremes, and near-term change remains limited.

Global climate models provide essential information on future climate change, but their precipitation skill over South Asia remains uneven, particularly for convective and regional-scale rainfall (Eyring et al., 2016; Moon and Ha, 2020; Guilbert et al., 2023; Kushwaha et al., 2024). Therefore, local applications should not rely on unexamined model outputs. Objective model screening, bias-aware interpretation, and explicit validation are needed before climate model information is translated into district-scale rainfall projections.

Machine learning can support this translation by learning nonlinear relationships between climate-model predictors and observed rainfall. However, ML applications in climate studies are vulnerable to overfitting, information leakage, and overstatement of predictive skill if chronological validation and uncertainty reporting are weak (Maraun et al., 2018; Reichstein et al., 2019; Beucler et al., 2021). In this study, ML is therefore treated as a post-processing and projection-mapping tool applied to already bias-corrected and statistically downscaled NEX-GDDP-CMIP6 data, not as primary dynamical downscaling.

The objectives are to: (i) characterize district-scale MAM rainfall variability and extremes from 1951 to 2024; (ii) evaluate and rank CMIP6 models using a composite performance index; (iii) compare RF, XGBoost, and LSTM models under chronological validation; and (iv) estimate near-term MAM rainfall changes for 2031-2050 under SSP5-8.5 in six selected districts of Telangana.

Material and Methods

Study area and observed rainfall

The analysis focuses on six districts representing contrasting hydroclimatic settings in Telangana: Adilabad, Nizamabad, Karimnagar, Hyderabad, Mahabubnagar, and Khammam (Figure 1). Daily gridded rainfall data at 0.25 deg x 0.25 deg resolution were obtained from the India Meteorological Department for 1951-2024 (Pai et al., 2021). Grid cells falling within each district boundary were spatially averaged to produce district-level daily series. Seasonal MAM totals were computed by summing daily rainfall, and wet-day frequency was defined using the IMD threshold of >=2.5 mm day^{-1}.

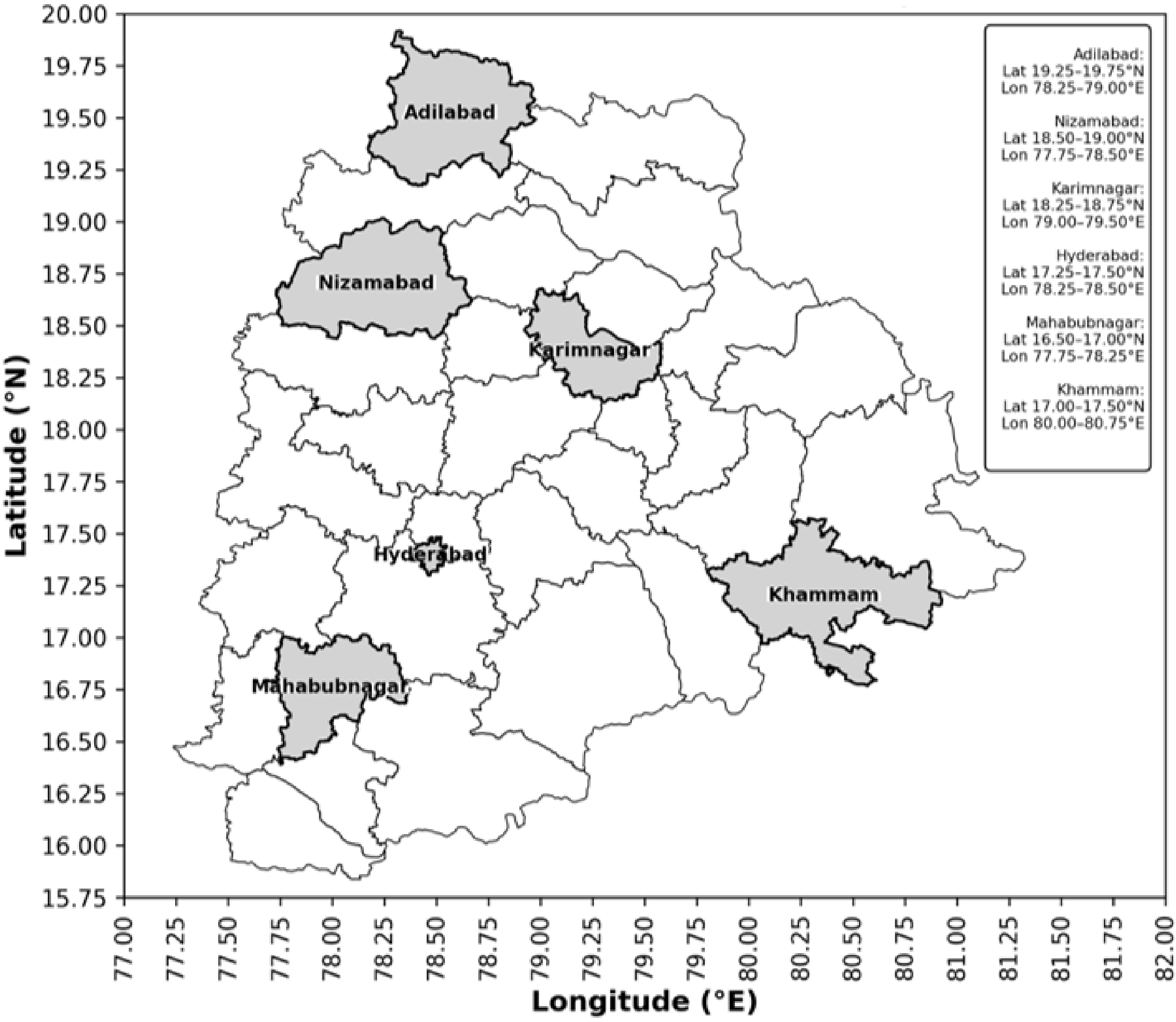

Figure 1. Location of the six selected districts in Telangana, India.

Observational diagnostics

Interannual variability was described using the coefficient of variation (CV = 100 x sigma/mu), where sigma and mu are the standard deviation and mean of seasonal rainfall. Rainfall concentration within the MAM season was assessed using the precipitation concentration index (PCI). Heavy rainfall was summarized using R10 and R20 (numbers of days with rainfall >=10 and >=20 mm), and R95p, defined as seasonal rainfall accumulated on days exceeding the 95th percentile threshold calculated from the 1951-2014 reference period (Zhang et al., 2011). Long-term monotonic trends were tested using the Mann-Kendall test and Sen's slope estimator (Mann, 1945; Kendall, 1957; Sen, 1968). Potential abrupt shifts were examined using the Pettitt test. To separate the mechanisms of rainfall change, wet-day frequency and rainfall intensity (rainfall per wet day) were analyzed separately.

CMIP6 data and model screening

Bias-corrected and statistically downscaled daily precipitation was obtained from the NASA NEX-GDDP-CMIP6 archive at 0.25 deg x 0.25 deg resolution (Thrasher et al., 2022). NEX-GDDP-CMIP6 uses a bias-correction and spatial-disaggregation lineage developed for climate-impact applications, so the ML component in this study is treated as post-processing rather than primary downscaling (Wood, 2002; Maurer and Hidalgo, 2008; Thrasher et al., 2012). Historical simulations for 1951-2014 were evaluated against IMD observations, while SSP5-8.5 projections were used for 2031-2050. Precipitation was converted from kg m^{-2} s^{-1} to mm day^{-1} by multiplying by 86,400 and then aggregated to monthly MAM totals. Twenty models were considered: ACCESS-CM2, ACCESS-ESM1-5, BCC-CSM2-MR, CMCC-CM2-SR5, CMCC-ESM2, EC-Earth3, EC-Earth3-Veg-LR, FGOALS-g3, GFDL-CM4, GISS-E2-1-G, INM-CM4-8, INM-CM5-0, IPSL-CM6A-LR, KIOST-ESM, MIROC-ES2L, MIROC6, MPI-ESM1-2-HR, MRI-ESM2-0, NorESM2-MM, and TaiESM1.

Model screening used four standard diagnostics for hydroclimatic model evaluation: Pearson correlation (r), normalized root mean square error (NRMSE), standard deviation ratio, and mean bias (Ramsey, 1996). Each metric was transformed so that lower values denoted better performance; correlation was converted to an error component as 1^{-r}, variability was measured as the absolute deviation of the standard deviation ratio from 1, and NRMSE and absolute bias were normalized across the candidate models. The composite performance index (CPI) was calculated as the arithmetic mean of these four normalized components. Models were ranked using the state-average CPI across the six districts.

Machine-learning post-processing and projection

RF, XGBoost, and LSTM models were trained using monthly MAM rainfall totals, representing tree-ensemble, gradient-boosting, and recurrent deep-learning approaches, respectively (Hochreiter and Schmidhuber, 1997; Breiman, 2001; Chen and Guestrin, 2016). Predictors were the district-level monthly precipitation series from the five selected CMIP6 models, and the target was IMD rainfall. A chronological split was used to reduce information leakage: 1951-2000 for training, 2001-2014 for validation and tuning, and 2015-2024 for independent testing. Scaling parameters were estimated from the training set only and then applied to validation and test periods. For post-2014 testing, the same predictor construction was applied to available scenario-period NEX-GDDP-CMIP6 data and compared with IMD observations; this evaluates the statistical post-processing framework under chronological holdout conditions and is not interpreted as deterministic year-by-year climate prediction.

RF used 400 trees, maximum depth 12, minimum split size 8, and minimum leaf size 4. XGBoost used 500 boosting rounds, learning rate 0.05, maximum depth 5, subsampling of 0.8 for rows and columns, minimum child weight 5, and early stopping. LSTM used a sequence-to-one structure with two stacked layers (64 and 32 units), dropout of 0.2, L2 regularization, Adam optimization, mean-squared-error loss, early stopping, and learning-rate scheduling. Model performance was evaluated using RMSE, MAE, R^2, correlation, and bias. Future MAM rainfall was projected for 2031-2050 under SSP5-8.5 relative to the 1981-2010 baseline. The reported 5-95%

range represents the spread of projected seasonal estimates over the 2031-2050 period; it should not be read as full scenario or structural model uncertainty.

Results

Observed rainfall variability and extremes

Observed MAM rainfall shows marked interannual variability in all six districts (Figure 2). Seasonal totals and wet-day counts do not always vary proportionally, indicating that high seasonal rainfall can result from a small number of intense events rather than from more frequent rainfall. Khammam records the most pronounced peaks, including years above 300-400 mm, whereas Hyderabad shows comparatively lower interannual variability despite episodic rainfall spikes.

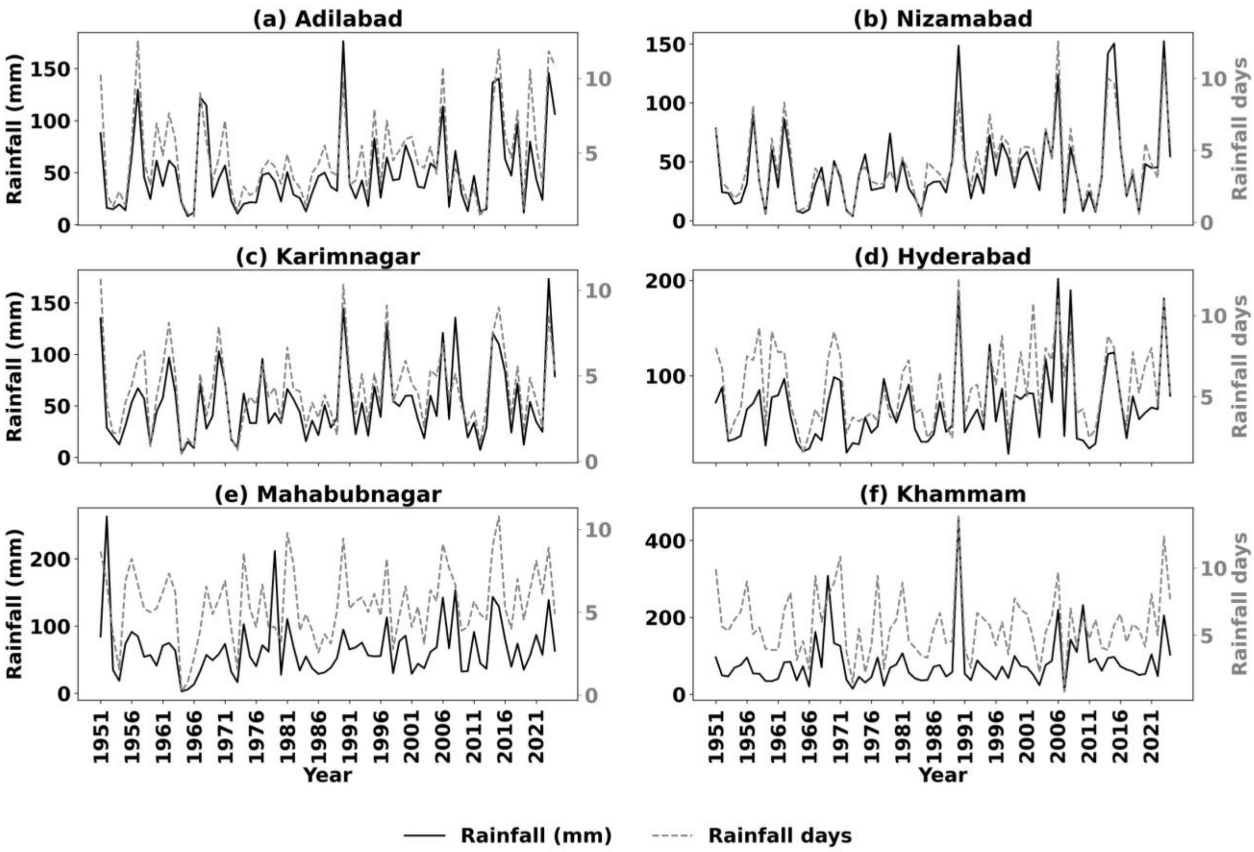

Figure 2. Observed MAM rainfall totals and wet-day frequency in the six districts, 1951-2024.

CV values exceed 60% in all districts, confirming the inherently unstable character of pre-monsoon rainfall (Figure 3A). Khammam has the highest CV (83.0%), followed by Nizamabad (78.5%) and Adilabad (74.2%); Hyderabad has the lowest CV (60.2%). PCI follows a similar spatial pattern, with the highest concentration in Khammam (2.27) and the lowest in Hyderabad (1.84). Thus, districts with larger year-to-year variability also tend to show stronger seasonal concentration.

Trend decomposition indicates that rainfall intensity has increased more consistently than wet-day frequency (Figure 3B). Nizamabad shows the strongest significant increase in rainfall days (0.028 days yr^{-1}), while Khammam shows almost no frequency change but the strongest significant increase in rainfall intensity (0.052 mm day^{-1} yr^{-1}). This pattern supports an intensity-dominated interpretation of recent MAM rainfall change.

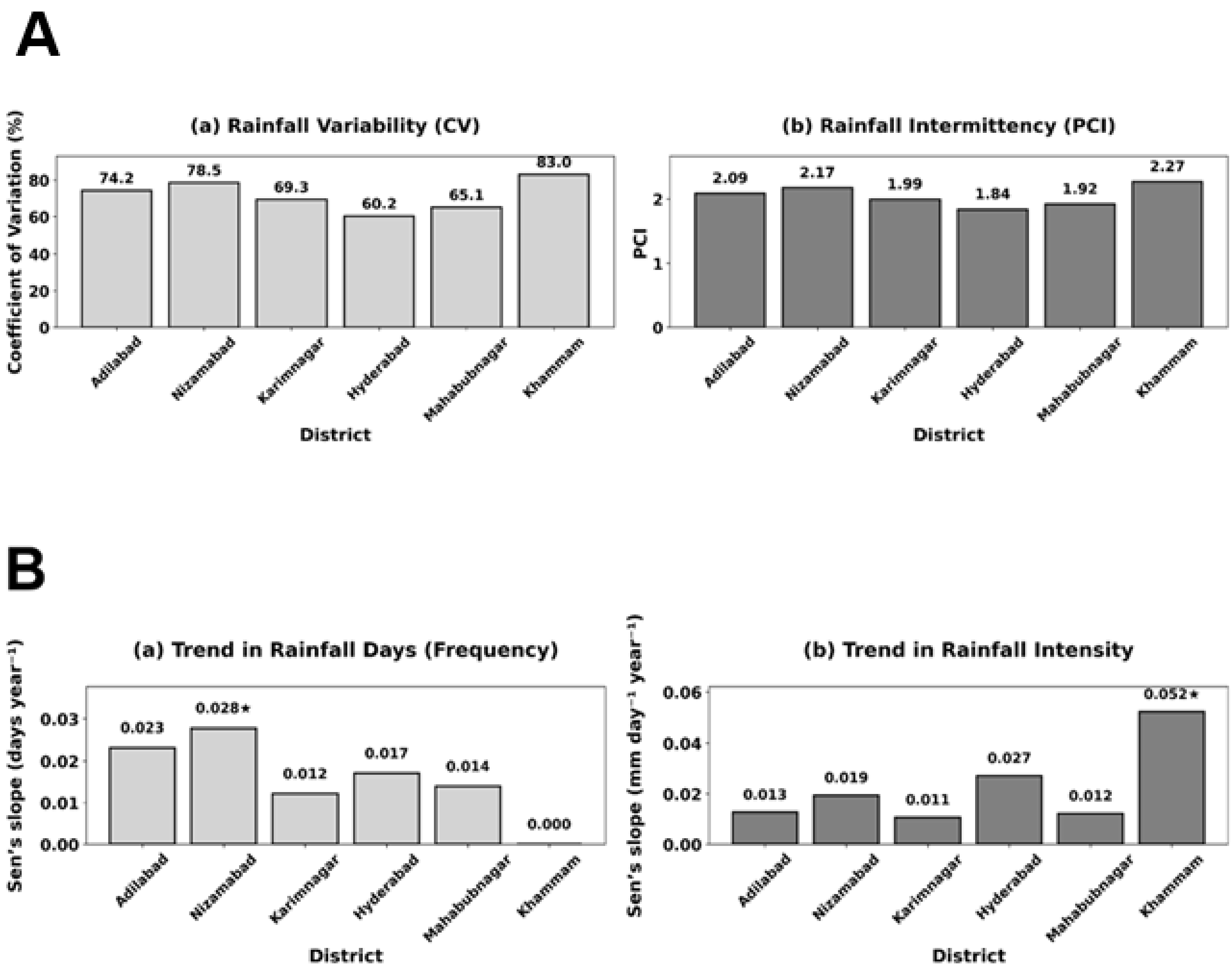

Figure 3. Rainfall variability, concentration, and intensity-frequency trends during MAM.

Seasonal rainfall trends are positive in all districts but are not uniformly significant (Figure 4A). Nizamabad and Khammam show the largest slopes (about 0.32 mm yr^{-1}), followed by Adilabad (0.30 mm yr^{-1}) and Hyderabad (0.28 mm yr^{-1}). Pettitt tests suggest possible shifts between the late 1980s and early 2000s, but none are statistically significant at $p<0.05$. Heavy rainfall diagnostics further indicate increasing contribution from very wet days, particularly in Khammam, supporting the conclusion that intensification rather than regime-shift behaviour dominates the observed signal (Figure 4B).

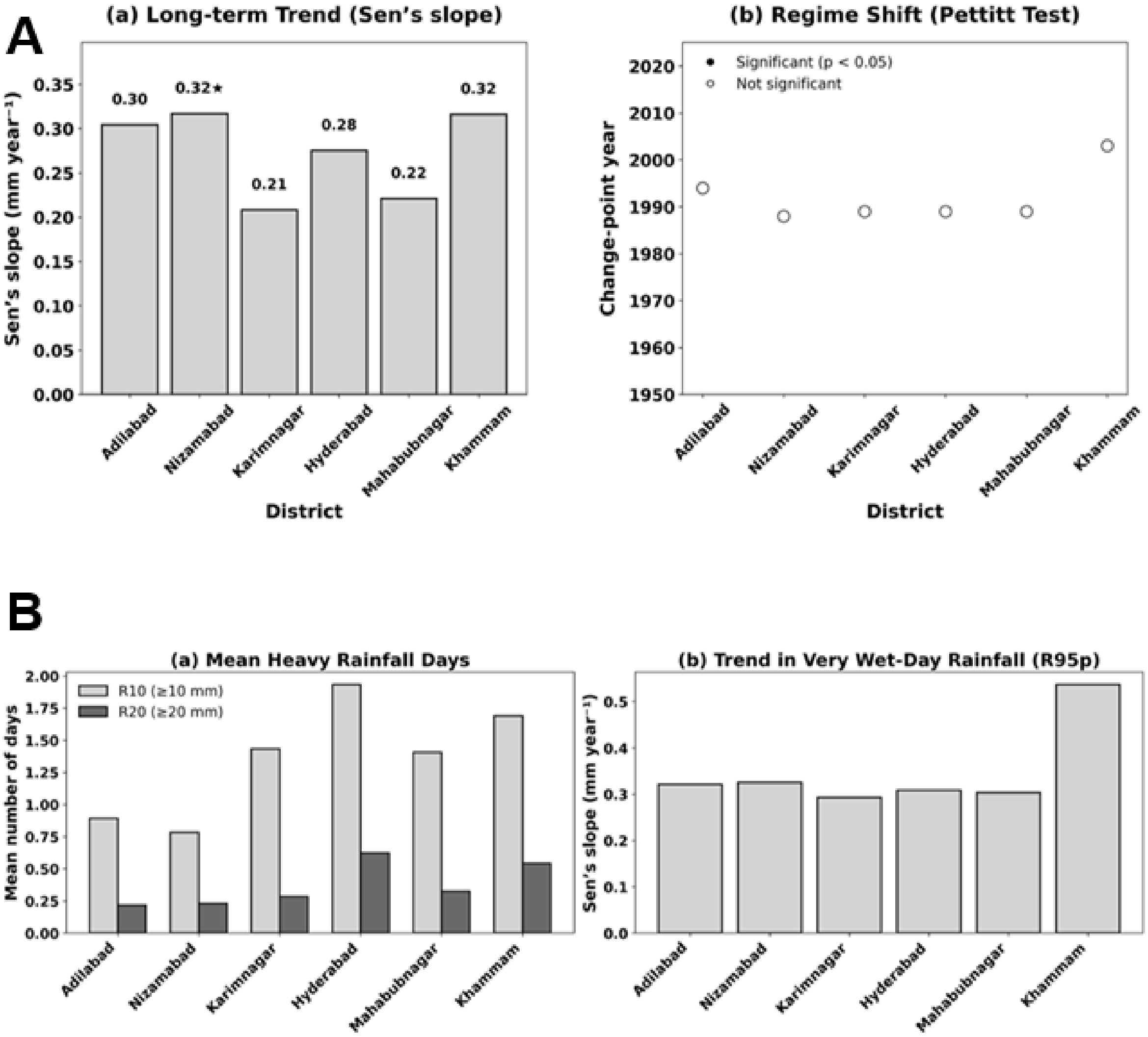

Figure 4. Long-term rainfall trends, Pettitt change-points, and heavy-rainfall diagnostics.

CMIP6 model performance

CMIP6 performance varies across both metrics and districts. No model is best for all diagnostics, which justifies a composite rather than single-metric screening strategy. The CPI ranking identifies five comparatively stable models for subsequent ML post-processing: CMCC-ESM2, ACCESS-ESM1-5, TaiESM1, MRI-ESM2-0, and INM-CM5-0 (Table 1; Figure 5). Their state-average CPI values range from 0.43 to 0.46, whereas the weakest models show state-average CPI near 0.59.

Table 1. Top five CMIP6 models retained for ML post-processing based on state-average CPI.

Rank	Selected CMIP6 model	State-average CPI
1	CMCC-ESM2	0.43
2	ACCESS-ESM1-5	0.43
3	TaiESM1	0.44
4	MRI-ESM2-0	0.45
5	INM-CM5-0	0.46

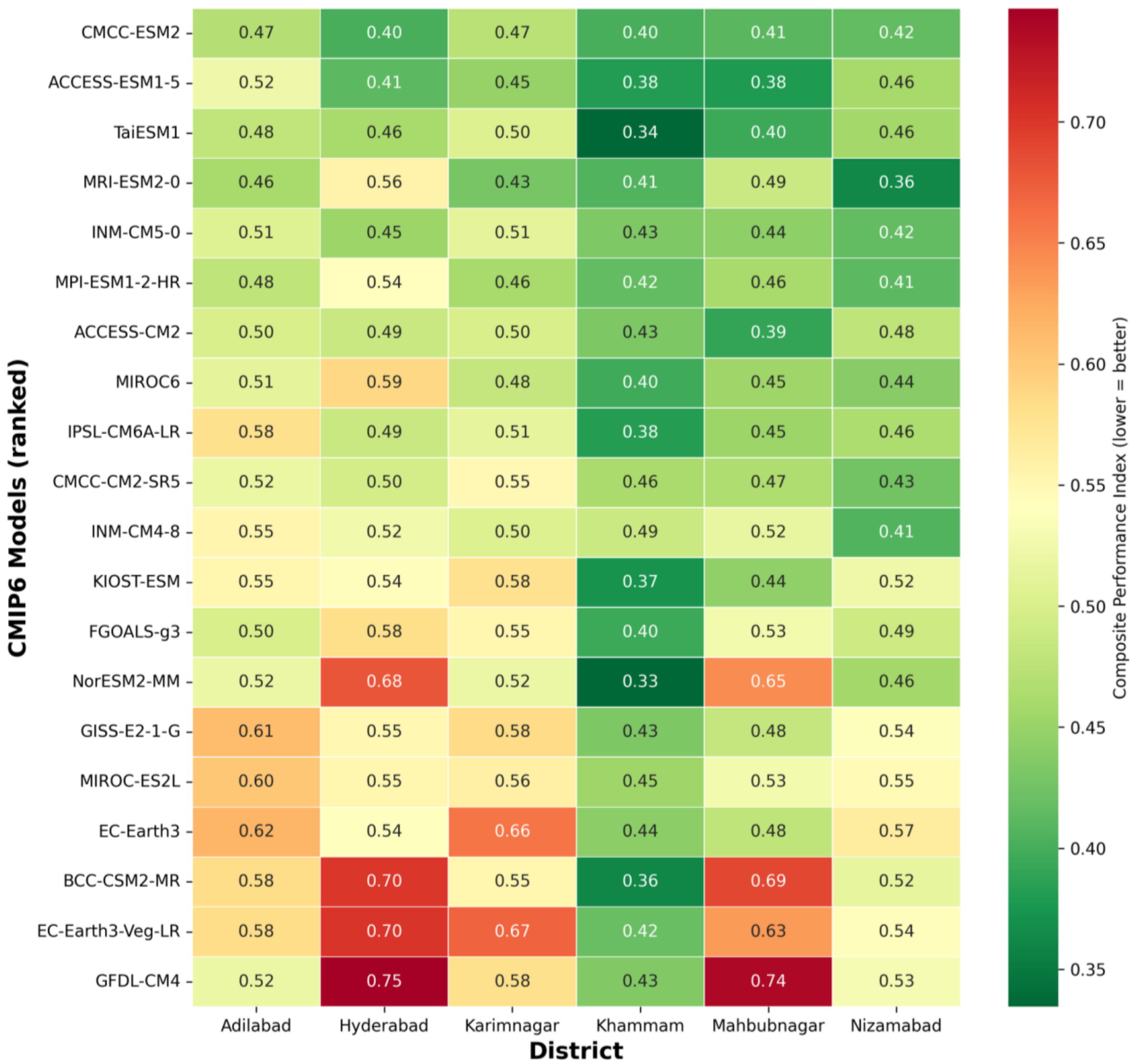

Figure 5. District-wise CPI ranking of CMIP6 models for historical MAM rainfall.

Machine-learning performance

The three ML algorithms provide broadly comparable predictive skill, but their error structures differ (Table 2; Figure 6). RF has the lowest mean RMSE across districts (74.63 mm), while LSTM has the highest mean R^2 (0.62) and correlation (0.79). XGBoost performs slightly weaker overall. Therefore, LSTM is not selected because it minimizes every error metric; rather, it is retained as the projection model because it provides the most stable association with observed interannual variability while reducing inter-district inconsistency. This distinction is important because LSTM still underestimates peak rainfall years, especially in high-intensity events.

Table 2. Mean independent-test performance across the six districts for 2015-2024.

Model	Mean RMSE (mm)	Mean MAE (mm)	Mean R^2	Mean r	Mean bias (mm)
RF	74.63	43.48	0.59	0.77	-6.95
XGBoost	84.42	50.30	0.56	0.75	-4.08
LSTM	78.73	47.83	0.62	0.79	-11.80

Comparative monthly-scale performance during the independent test period is summarized in Figure 6. RF, XGBoost, and LSTM show broadly comparable error distributions, although RF has a slightly lower median RMSE in some districts. LSTM does not consistently produce the lowest errors, but its narrower spread indicates more stable performance across heterogeneous district rainfall regimes. Therefore, LSTM was retained as the primary projection model on the basis of consistency rather than absolute error minimization.

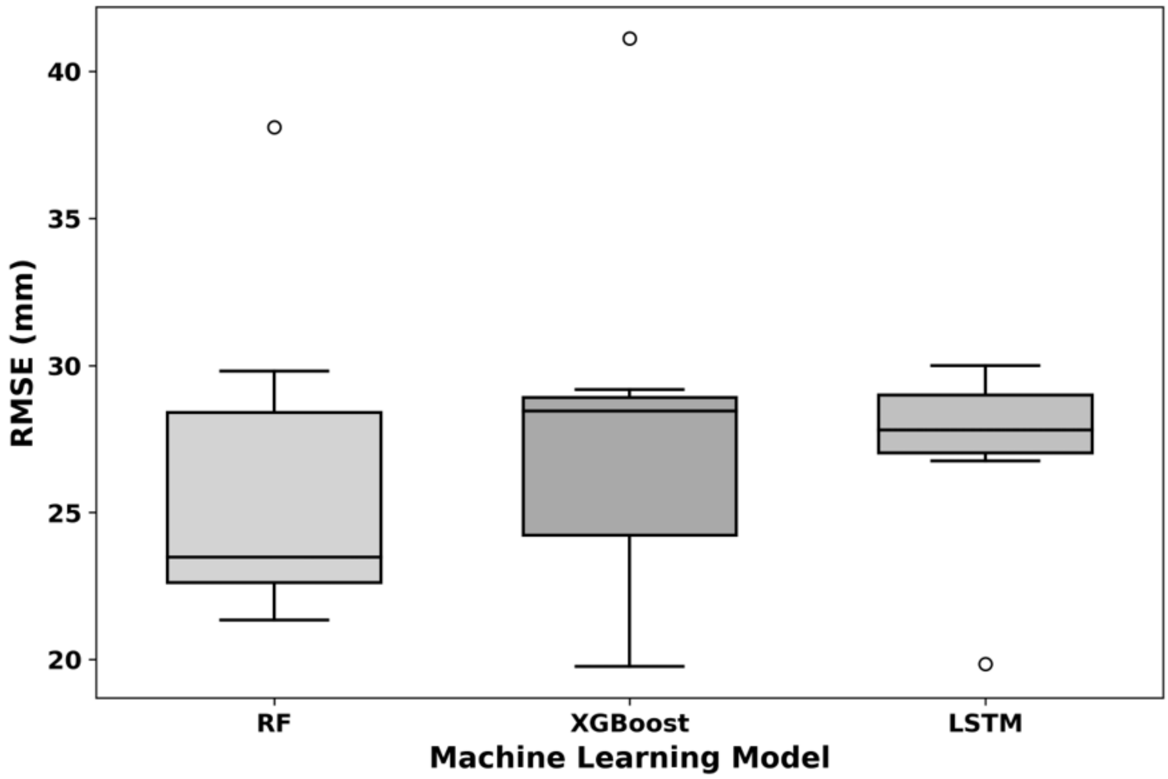

Figure 6. Monthly RMSE comparison of RF, XGBoost, and LSTM models during independent testing (2015-2024).

Seasonal validation of the selected LSTM model is shown in Figure 7. The model follows wet–dry phasing in most districts but smooths the amplitude of anomalously wet years. Seasonal RMSE values range from 43.1 mm in Mahabubnagar to 64.3 mm in Nizamabad, with intermediate errors in Khammam (49.4 mm), Hyderabad (52.7 mm), Karimnagar (61.3 mm), and Adilabad (62.8 mm). These results indicate useful seasonal-scale tracking of rainfall variability, but also confirm persistent underestimation of peak rainfall years.

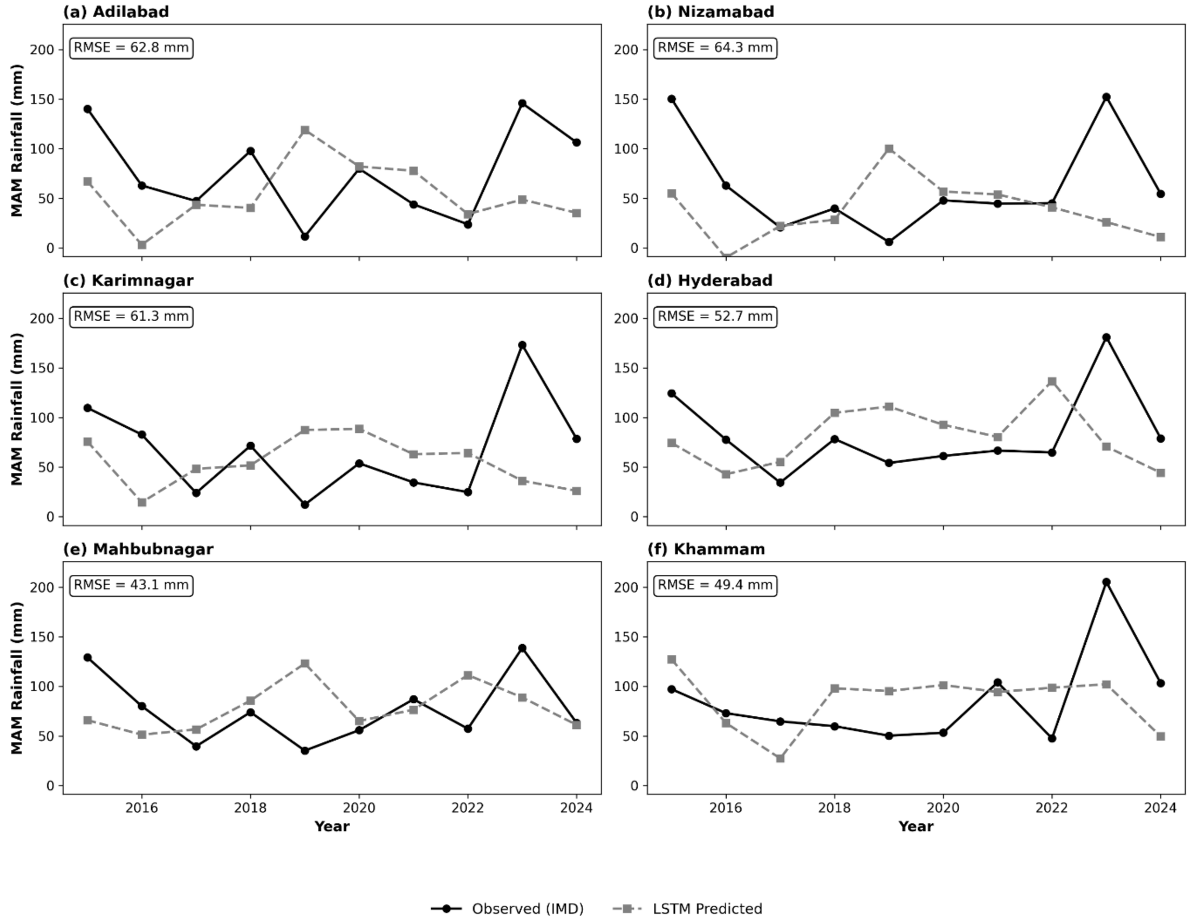

Figure 7. Seasonal validation of the selected LSTM model against IMD observations across six districts (2015-2024).

Near-term projection under SSP5-8.5

LSTM-based projections for 2031-2050 indicate spatially heterogeneous MAM rainfall change relative to 1981-2010 (Table 3; Figure 8). Adilabad has the largest projected increase (+36.35%), followed by Karimnagar (+19.90%), Hyderabad (+10.99%), and Mahabubnagar (+7.72%). Khammam remains nearly unchanged, while Nizamabad shows a modest decline (-5.21%). Projected mean seasonal rainfall is highest in Khammam (~88 mm) and Hyderabad (~81 mm) and lowest in Nizamabad (~43 mm). The wide 5-95% range indicates that internal variability remains large even during the near-term projection period.

Table 3. LSTM-based near-term MAM rainfall projection for 2031-2050 under SSP5-8.5.

District	Projected change (%)	Projected mean MAM rainfall (mm)
Adilabad	+36.35	~65
Nizamabad	-5.21	~43
Karimnagar	+19.90	~66
Hyderabad	+10.99	~81
Mahabubnagar	+7.72	~68
Khammam	~0	~88

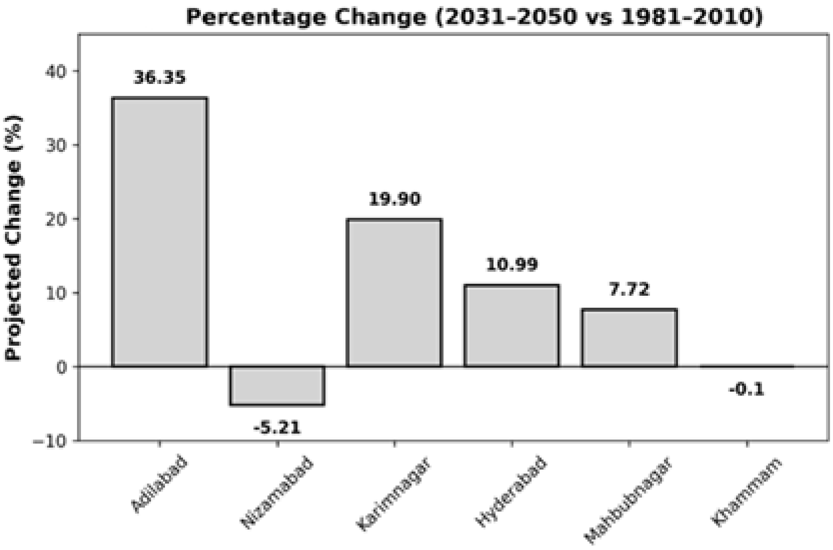

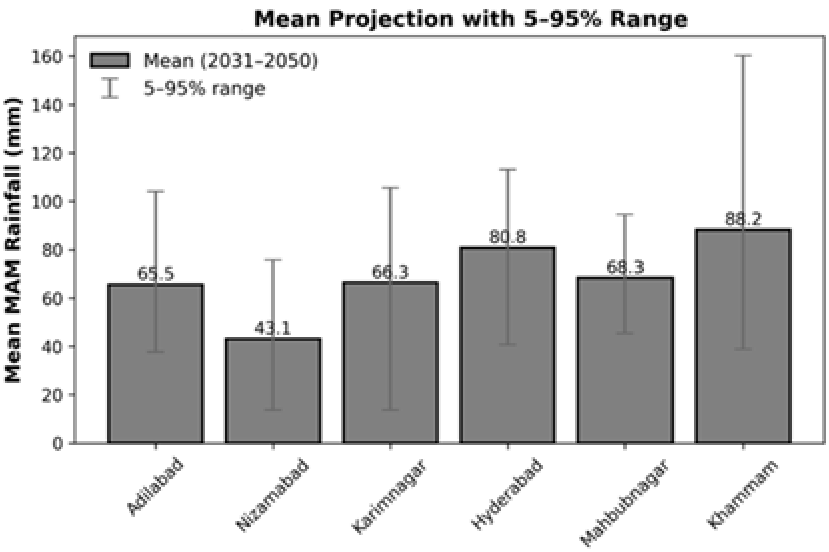

Figure 8. Projected MAM rainfall change and 5-95% interannual spread for 2031-2050 under SSP5-8.5.

Discussion

The observed results indicate that MAM rainfall change in the selected districts is better described as intensification than as a uniform increase in rainy-day frequency. This interpretation is consistent with the convective nature of pre-monsoon rainfall over peninsular India, where short-duration storms can dominate seasonal totals (Houze et al., 2007; Turner and Annamalai, 2012). It also agrees with evidence for increasing heavy-rainfall intensity over India under recent warming (Goswami et al., 2006; Roxy et al., 2017; Mukherjee et al., 2018). The evidence is strongest in Khammam, where rainfall intensity and extreme-rainfall contribution increase despite nearly stable wet-day frequency. However, not all district-level trends are statistically significant, so the results should be interpreted as spatially heterogeneous evidence rather than a state-wide monotonic signal.

The absence of significant Pettitt change-points suggests gradual evolution rather than abrupt regime shifts. This matters for adaptation because gradual intensification can still increase runoff, reduce rainfall-use efficiency, and raise urban flood risk, particularly where high rainfall is concentrated into fewer events. The agricultural relevance is also clear because pre-monsoon rainfall affects soil moisture, groundwater recharge, and early-season crop planning in rain-fed systems (Gadgil and Gadgil, 2006; Kumar et al., 2004). Hyderabad's relatively low CV therefore does not remove risk; its urban exposure means even moderate intensification can have disproportionate consequences.

The CMIP6 evaluation confirms that model skill is metric- and location-dependent, which is consistent with known difficulties in representing South Asian precipitation and convective rainfall in global climate models (Eyring et al., 2016; Moon and Ha, 2020; Guilbert et al., 2023; Kushwaha et al., 2024). A composite screening approach is therefore justified, but it does not eliminate uncertainty. CPI gives a transparent basis for selecting predictors, yet it depends on normalization choices and equal weighting. The selected models should be viewed as historically better-performing candidates, not as a definitive ensemble of future truth.

The ML results are useful but should not be oversold. RF, XGBoost, and LSTM achieve comparable skill, and RF has lower mean RMSE in the independent test period. LSTM is retained mainly because of its stronger mean correlation and relatively stable representation of temporal variability, a feature consistent with the ability of recurrent/deep-learning methods to represent nonlinear temporal dependencies in climate data (Hochreiter and Schmidhuber, 1997; Reichstein et al., 2019; Baño-Medina et al., 2020; Chen et al., 2023). Its tendency to underestimate extremes is a critical limitation for pre-monsoon rainfall, where rare events strongly influence seasonal totals. This limitation echoes broader concerns that data-driven climate models require careful validation, physical constraints, and uncertainty treatment before they are used for impact assessment (Maraun et al., 2018; Beucler et al., 2021). Daily or sub-daily predictors, moisture flux, instability indices, and circulation diagnostics would likely improve representation of convective extremes.

Projection results under SSP5-8.5 point to localized increases rather than uniform wetting across Telangana. The strongest projected increase in Adilabad and the decline in Nizamabad demonstrate why aggregated state-level projections can be misleading. This is particularly important for near-term planning, where internal variability and regional model spread can strongly shape the emergence of climate signals (Hawkins and Sutton, 2012; Meehl et al., 2014). Because only one forcing pathway is used and the 5-95% range represents interannual spread rather than full structural uncertainty, these projections should support risk-aware planning rather than deterministic local forecasts.

Conclusion

This study provides a compact district-scale assessment of pre-monsoon rainfall variability, CMIP6 model performance, and near-term ML-based projection for six contrasting districts of Telangana. Observations from 1951-2024 show high variability in all districts, with CV values above 60% and strongest variability in Khammam. Trend decomposition indicates that rainfall change is more strongly linked to event intensity than to wet-day frequency, although statistical significance is not uniform across districts. CMIP6 screening with a composite performance index identified CMCC-ESM2, ACCESS-ESM1-5, TaiESM1, MRI-ESM2-0, and INM-CM5-0 as the most suitable predictors for post-processing. RF, XGBoost, and LSTM showed comparable validation skill; LSTM was retained for projections because it better preserved temporal association across districts, not because it eliminated errors. Its underestimation of extreme wet years remains a major limitation. Under SSP5-8.5, projected MAM rainfall changes for 2031-2050 is spatially heterogeneous, ranging from -5.2% in Nizamabad to +36.4% in Adilabad. These findings argue for district-specific planning and caution against broad state-level generalization. Future work should use higher-frequency predictors, additional atmospheric variables, and multi-scenario probabilistic frameworks to improve the representation of convective rainfall extremes.

Acknowledgments

The authors acknowledge the Department of Meteorology and Oceanography, Andhra University; the National Institute of Disaster Management (NIDM), South Campus; and the Centre for Atmospheric Science, Koneru Lakshmaiah Education Foundation. The authors also acknowledge the India Meteorological Department and the CMIP6 modelling groups for making the datasets used in this study available.

Author Contributions

G.J.M. performed data curation, formal analysis, visualization, and original draft preparation. G.C.S. provided conceptual guidance, supervision, and review and editing. S.V. contributed to methodology, software, analysis, and review and editing. C.V.N. provided supervision and review and editing. M.A.K. contributed to machine-learning methodology, statistical analysis, and review and editing. M.P.R. supported data collection and analysis.

Funding Statement

The authors declare that no specific grant from any funding agency in the public, commercial, or not-for-profit sectors supported this work.

Conflict of Interest Statement

The authors declare that they have no conflict of interest.

Ethical Approval Statement

No ethics committee permissions are required for this study.

Data Availability Statement

IMD gridded rainfall data are available through the India Meteorological Department data portal. CMIP6 downscaled projections were obtained from the NASA NEX-GDDP-CMIP6 archive. Access is subject to the policies of the respective data providers.

References

Baño-Medina, J., Manzanas, R., Gutiérrez, J.M. (2020). Configuration and Intercomparison of Deep Learning Neural Models for Statistical Downscaling. Geoscientific Model Development, 13, 2109-2124, doi: 10.5194/gmd-13-2109-2020

Beucler, T., Pritchard, M., Rasp, S., Ott, J., Baldi, P., Gentine, P. (2021). Enforcing Analytic Constraints in Neural Networks Emulating Physical Systems. Physical Review Letters, 126. doi: 10.1103/physrevlett.126.098302

Breiman, L. (2001). Random forests. Machine Learning, 45, 5-32.

Chen, L., Han, B., Wang, X., Zhao, J., Yang, W., Yang, Z. (2023). Machine Learning Methods in Weather and Climate Applications: A Survey. Applied Sciences, 13(21), 12019, doi: 10.3390/app132112019

Chen, T., Guestrin, C. (2016). XGBoost: A Scalable Tree Boosting System. *In*: The Proceeding Book of the 22nd ACM SIGKDD International Conference on Knowledge Discovery and Data Mining, California, USA, 785-794, doi: 10.1145/2939672.2939785

Eyring, V., Bony, S., Meehl, G.A., Senior, C.A., Stevens, B., Stouffer, R.J., Taylor, K.E. (2016). Overview of the Coupled Model Intercomparison Project Phase 6 (CMIP6) Experimental Design and Organization. Geoscientific Model Development, 9(5), 1937-1958, doi: 10.5194/gmd-9-1937-2016

Gadgil, S., Gadgil, S. (2006). The Indian Monsoon, GDP and Agriculture. Economic and Political Weekly, 4887-4895, doi: 10.2307/4418949

Goswami, B.N., Venugopal, V., Sengupta, D., Madhusoodanan, M.S., Xavier, P.K. (2006). Increasing Trend of Extreme Rain Events Over India in a Warming Environment. Science, 314(5804), 1442-1445, doi: 10.1126/science.1132027

Guilbert, M., Terray, P., Mignot, J. (2023). Intermodel spread of historical Indian monsoon rainfall change in CMIP6: the role of the tropical Pacific mean state. Journal of Climate, 36, 3937-3953, doi: 10.1175/jcli-d-22-0585.1

Hawkins, E., Sutton, R. (2012). Time of Emergence of Climate Signals. Geophysical Research Letters 39, L01702, doi: 10.1029/2011gl050087

Hochreiter, S., Schmidhuber, J. (1997). Long Short-Term Memory. Neural Computation, 9, 1735-1780, doi: 10.1162/neco.1997.9.8.1735

Houze, R.A., Wilton, D.C., Smull, B.F. (2007). Monsoon Convection in the Himalayan Region as Seen by the TRMM Precipitation Radar. Quarterly Journal of the Royal Meteorological Society, doi: 10.1002/qj.106

Kendall, M.G. (1957). Rank Correlation Methods. Biometrika, 44, 298, doi: 10.2307/2333282

Krishnan, R., Sanjay, J., Gnanaseelan, C., Mujumdar, M., Kulkarni, A., Chakraborty, S. (2020). Assessment of climate change over the Indian Region. A report of the Ministry of Earth Sciences (MoES), Government of India. Springer Singapore.

Kumar, K., Kumar, K., Ashrit, R.G., Deshpande, N.R., Hansen, J.W. (2004). Climate Impacts on Indian Agriculture. International Journal of climatology, 24(11), 1375-1393, doi: 10.1002/joc.1081

Kushwaha, P., Pandey, V.K., Kumar, P., Sardana, D. (2024). CMIP6 Model Evaluation for Mean and Extreme Precipitation Over India. Pure and Applied Geophysics, 181, 655-678. doi: 10.1007/s00024-023-03409-5

Mann, H.B. (1945). Nonparametric Tests Against Trend. Econometrica, 13, 245, doi: 10.2307/1907187

Maraun, D., Widmann, M., Gutiérrez, J.M. (2018). Statistical Downscaling Skill Under Present Climate Conditions: A Synthesis of the VALUE Perfect Predictor Experiment. International Journal of Climatology, 39, 3692-3703, doi: 10.1002/joc.5877

Maurer, E.P., Hidalgo, H.G. (2008). Utility of Daily vs. monthly large-scale climate data: An Intercomparison of Two Statistical Downscaling Methods. Hydrology and Earth System Sciences, 12, 551-563, doi: 10.5194/hess-12-551-2008

Meehl, G.A., Goddard, L., Boer, G., Burgman, R., Branstator, G., Cassou, C., Corti, S., Danabasoglu, G., Doblas-Reyes, F., Hawkins, E., Karspeck, A., Kimoto, M., Kumar, A., Matei, D., Mignot, J., Msadek, R., Navarra, A., Pohlmann, H., Rienecker, M., Rosati, T., Schneider, E., Smith, D., Sutton, R., Teng, H., Jan van Oldenborgh, G., Vecchi, G., Yeager, S. (2014). Decadal Climate Prediction: An Update from the Trenches. Bulletin of the American Meteorological Society, 95, 243-267, doi: 10.1175/bams-d-12-00241.1

Moon, S., Ha, K-J. (2020). Future Changes in Monsoon Duration and Precipitation Using CMIP6. npj Climate and Atmospheric Science 3(1), 45, doi: 10.1038/s41612-020-00151-w

Mukherjee, S., Aadhar, S., Stone, D., Mishra, V. (2018). Increase in Extreme Precipitation Events Under Anthropogenic Warming in India. Weather and Climate Extremes, 20, 45-53, doi: 10.1016/j.wace.2018.03.005

Pai, D.S., Rajeevan, M., Sreejith, O.P., Mukhopadhyay, B., Satbha, N.S. (2014). Development of a new high spatial resolution (0.25× 0.25) long period (1901-2010) daily gridded rainfall data set over India and its comparison with existing data sets over the region. Mausam, 65(1), 1-18, doi: 10.54302/mausam.v65i1.851

Ramsey, P.H. (1996). Statistical Methods in the Atmospheric Sciences. Technometrics, 38(4), 402, doi: 10.1080/00401706.1996.10484553

Reichstein, M., Camps-Valls, G., Stevens, B., Jung, M., Denzler, J., Carvalhais, N., Prabhat, F. (2019). Deep Learning and Process Understanding for Data-Driven Earth System Science. Nature, 566(7743), 195-204, doi: 10.1038/s41586-019-0912-1

Roxy, M.K., Ghosh, S., Pathak, A., Athulya, R., Mujumdar, M., Murtugudde, R., Terray, P., Rajeevan, M. (2017). A Threefold Rise in Widespread Extreme Rain Events Over Central India. Nature Communications, 8(1), 708, doi: 10.1038/s41467-017-00744-9

Sen, P.K. (1968). Estimates of The Regression Coefficient Based on Kendall's Tau. Journal of the American Statistical Association, 63(324), 1379-1389, doi:10.1080/01621459.1968.10480934

Thrasher, B., Maurer, E.P., McKellar, C., Duffy, P.B. (2012). Bias Correcting Climate Model Simulated Daily Temperature Extremes with Quantile Mapping. Hydrology and Earth System Sciences, 16(9), 3309-3314, doi: 10.5194/hess-16-3309-2012

Thrasher, B., Wang, W., Michaelis, A., Melton, F., Lee, T., Nemani, R. (2022). NASA Global Daily Downscaled Projections, CMIP6. Scientific Data, 9(1), 262, doi: 10.1038/s41597-022-01393-4

Turner, A.G., Annamalai, H. (2012). Climate Change and the South Asian Summer Monsoon. Nature Climate Change, 2, 587-595, doi: 10.1038/nclimate1495

Wood, A.W. (2002). Long-Range Experimental Hydrologic Forecasting for the Eastern United States. Journal of Geophysical Research, 107(D20), 4429, doi: 10.1029/2001jd000659

Zhang, X., Alexander, L., Hegerl, G.C., Jones, P., Tank, A.K., Peterson, T.C., Trewin, B., Zwiers, F. W. (2011). Indices for monitoring changes in extremes based on daily temperature and precipitation data. Wiley Interdisciplinary Reviews: Climate Change, 2(6), 851-870, doi: 10.1002/wcc.147